

Dynamics and motion control of a two pendulums driven spherical robot

Bo Zhao, Mantian Li, Haitao Yu, Haiyan Hu, Lining Sun

Abstract—This paper deals with the dynamics and motion control of a spherical robot designed for reconnaissance and unstructured hostile environment exploration. The robot in this paper has three DOFs and two inputs, of which the nature is a nonlinear and underactuated system with nonholonomic dynamic constraints. The improved construction of two pendulums offers novel motion principle of spherical robot, which is moving simultaneously actuated by both eccentric moment and inertial moment generated by the two pendulums. Meanwhile the mobility is enhanced when the robot behaves dynamically. The emphasis is placed on the linear motion and turning in place motion control. The dynamic model of linear motion is formulated on the basis of Lagrange equation, and a smooth trajectory planning method is proposed for linear motion. A feedback controller is constructed to ensure the accurate trajectory planning. Turning in place motion is an indispensable element of omni directional locomotion which can enhance the mobility of spherical robots. The dynamic model of turning in place motion is derived on the theory of moment of momentum, and a stick-slip principle is analyzed. The two motion control methods are validated by both simulations and prototype experiments.

I. INTRODUCTION

Traditionally, mobile robot is considered to be wheeled robot or legged robot. The wheeled robot features great mobility on relatively flat terrains, and the legged robot has potentially greater mobility on tough terrain [1]. In recent years, spherical robot, a new type of mobile robot, has attracted wide attention of researchers. Compared with wheeled or legged robots, besides great mobility on various terrains, spherical robot has the following advantages: (1) moving without roll-over problem, the stability can be restored by itself, the attitude is easy to recover after collision or falling down from the height; (2) the spherical robots can potentially move omnidirectionally with high dexterity, such as turning in place; (3) entire system is accommodated inside the ball-shaped shell, all devices are

protected by the outer shell [2]. So spherical robot can be used in hostile environments, such as rescue in disaster and military reconnaissance, especially planetary exploration. According to the differences of actuator, the representative spherical robots are grouped into six types: rotor type, car type, mobile masses type, gyroscope type, memory alloy type and pendulum type; each type has merits and demerits respectively [3]. The basic motion principle of the six types can be summarized as two kinds of motion principle; one is generating friction force by driving the device which is contact with the inner surface of the shell, such as rotor type and car type; the other is continuously changing the position of center of gravity of the robot by controlling the drive unit, such as mobile masses type, gyroscope type, memory alloy type and pendulum type. The former is applied in the early spherical robots; the latter is widely utilized by recent spherical robots, especially the pendulum type which is employed by most spherical robots. The “roball” spherical robot developed by Francois Michaud, the “BHQ” developed by ZhanQiang and the “GroundBot” developed by Mattias Seeman are all based on pendulum type [4]–[6]. The pendulum which is driven by two motors can rotate about the horizontal axis and the vertical axis, so the eccentric moment and inertia moment are generated, by which the robot can roll linearly or steer. The drawback of pendulum driven spherical robot is that the energy input of the motor for vertical rotation of pendulum is utilized only for steering, which is not an effective utilization of power supply. The researches on spherical robot in recent years mainly focus on trajectory planning and motion control [7]–[10], rather than motion principle and mechanism design. However, the linear motion and turning in place motion have not been proposed as the individual motion in previous researches on trajectory planning and motion control.

This paper deals with the dynamics and motion control of a spherical robot based on novel improved two pendulums type which engages novel motion principle. The drive mechanism of the robot in this paper differs from the previous designs. The linear motion control and turning in place motion control are studied respectively as two separate motions. The design details of the robot are described in Sec. II along with the motion principle. Section III provides linear motion control of the robot. The dynamic equation of the linear motion is formulated on constrained Lagrange method and principle of virtual work. Based on the dynamics, a smooth trajectory planning control method is proposed. A feedback controller is constructed for the accurate trajectory planning. The effectiveness of the method is validated by simulation and prototype experiment. Section IV provides the turning in place motion control. The

Manuscript received Mar. 10, 2010. This work was supported in part by High Technology Research Development Program of China (No.2005AA4202302) and the Program for Changjiang Scholars and Innovative Research Team in University (IRT0423).

Bo Zhao is with the State Key Laboratory of Robotics and System, Harbin Institute of Technology. Harbin, 150001 China (corresponding author to provide phone: 13674681656; fax: 0451-86402217; e-mail: hitzhaobo@gmail.com).

Mantian Li is with the State Key Laboratory of Robotics and System, Harbin Institute of Technology. Harbin, 150001 China (e-mail: limt@hit.edu.cn).

Haitao Yu is with the State Key Laboratory of Robotics and System, Harbin Institute of Technology. Harbin, 150001 China (e-mail: yukings1984@163.com).

dynamic equation is derived on the theory of moment of momentum. A stick-slip principle is interpreted in detail. The control method is verified by simulation, and the results of prototype experiment validate the effectiveness of the control method.

II. SYSTEM DESCRIPTION

A. Mechanical Structure

The mechanical structure of the robot is shown in Fig. 1, which is mainly composed of two motors, two pendulums, springs, linear bearings, two guides and the outer shell.

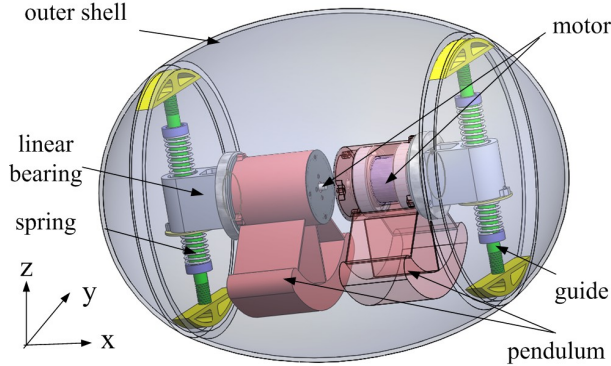


Fig. 1. Mechanical structure of the robot

The outer shell is ellipsoid, whose diameter of major axis is 176 mm, and the minor axis 146 mm. While in irregular motion, such as passing over bumps, the attitude of the robot is easy to be observed. Meanwhile, the pitch angle is restricted to a certain range by the ellipsoid shell, which ensures the robot can tolerate side slopes without rolling over.

A novel two pendulums type is adopted. The robot is driven by two pendulums placed diametrically opposite on the major axis of the ellipsoid shell, which are actuated by two direct current (DC) servomotors. The two pendulums can be only rotated about the major axis, which could change the position of the center of gravity of the robot and meanwhile afford the inertia force. This configuration brings a novel motion principle of spherical robot. The robot is motivated by eccentric moment, inertia force and inertia moment simultaneously. The total weight of the masses is 700 gram which accounts for 42.9% of the total mass of robot. Compared with the traditional pendulum type, the improved type can afford more eccentric moment and inertia force which make the robot has featured high speed, the ability of slope climbing and obstacle overcoming. The drive mechanism of the robot is composed of two motors and two pendulums which are connected to the linear guide by linear bearings whose two ends are pressed by springs. This elastic connection can buffer the impact when the robot falls down from the high or is in collision. And in the future works, the masses will be controlled to resonate with the springs in order to let the robot jump while in trap.

B. Motion Principle

As shown in Fig. 1, the spindle is along the x axis. The two pendulums can only rotate about the spindle to a tilt

angle θ , which results in the displacement of the center of gravity of the robot. The robot could only roll about the x axis under the action of the eccentric moment. Meanwhile the motor should keep rotating to maintain the angle θ for the continuous rotation about x axis, and the inertia forces are simultaneously generated by the acceleration of the pendulums, which are paralleled to yoz plane. The inertia forces could be decomposed into two orthogonal forces along y and z axes and one couple about x axis. Projected onto the yoz plane, the inertia forces along the y and z axes can afford inertia moment about the z and y axes respectively, so the robot could roll about the z and y axes. The inertia moment about the z axis is sufficient to activate the robot turning in place on relatively smooth ground. Because of static equilibrium of the moment about y axis and the restriction from the shape of outer shell, the robot can only roll about the y axis in a certain angle. The energy input is predominantly utilized for reacting against the friction force in slow or stable motion, and the inertia moment is significant with respect to eccentric moment in dynamically unstable motion.

C. Control system

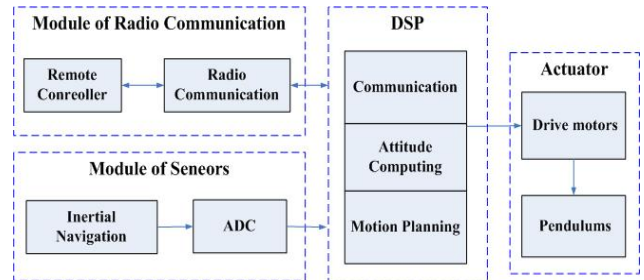


Fig. 2. Control system diagram of the robot

The two classes control system is designed because the robot belongs to a nonholonomic and under-actuated system. Fig. 2 is the control system diagram of the robot, which is composed of sensors, communication module, control module and actuators. The module of sensor consists of encoders of the servomotors, angular rate sensors, angular acceleration sensors and directional gyro, which are all micro electromechanical systems (MEMS) devices. An embedded control system is designed for attitude computing and motion planning. The operator can not directly control the pendulums to activate the robot, because the point-contact between outer shell and ground and small error in motions of the two pendulums may cause the unexpected motion of the robot. So the instructions for motion of robot sent by a remote controller should be “move straight” or “turn right for 20 degree”. The data of encoders, angular rate sensor and directional gyro are processed by attitude computing algorithms to get the current attitude of robot. The instructions for motors are computed by motion planning algorithms and then sent to actuators.

III. LINEAR MOTION CONTROL

A. Dynamic model of linear motion

In linear motion, the robot can be projected onto side view, which is modeled as a pendulum inside a rigid sphere

unrelated to the ellipsoid shell as shown in Fig. 3. The dynamics of the robot is derived under the following assumptions: (i) there is no slip between the shell and floor. (ii) the two pendulums rotate synchronously without angle difference.

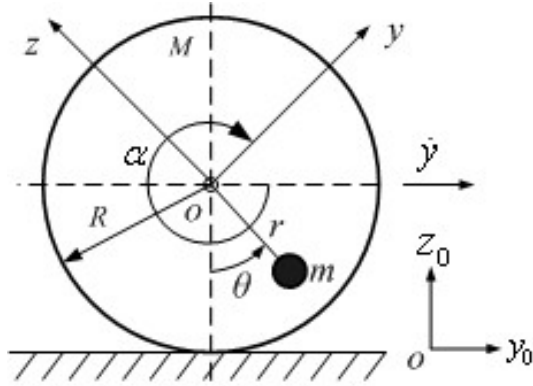


Fig. 3. Planar simplified model of linear motion

As shown in Fig. 3, the coordinate y_0oz_0 is considered to be reference coordinates fixed to the ground, and the coordinate yoz is fixed to the robot. The two pendulums are rotated by motors to a θ angle to change the position of center of the sphere. Additionally the inertia forces in yoz plane perpendicular to the pendulums are generated. The sphere rolls about the x axis driven by the eccentric moment and inertia moment from the two pendulums, so the center of the sphere moves straightly along the y_0 axis. The locomotion should be maintained by the continuous rotation of the two pendulums. The Lagrange equations are used to derive the dynamic equations of linear motion. The angle between the pendulums and vertical is referred as the tilt angle θ . The angle the sphere rotates through with respect to the reference coordinates is the body angle α . So the angle the motor shafts rotates through is $\theta + \alpha$. The tilt angle θ and distance of the center of the sphere y are considered to be the generalized coordinates in Lagrange equations, and the torque of the motors τ is the generalized force.

The kinetic energy of the sphere except for pendulums respect to ground can be expressed as

$$T_1 = \frac{1}{2} M \dot{y}^2 + \frac{1}{2} J \dot{\alpha}^2 \quad (1)$$

where M is the mass of the sphere, $J = MR^2$ is the moment of inertia of the sphere, R is the sphere radius, $\dot{y} = \dot{\alpha}R$ is the forward speed of the center of the sphere.

The kinetic energy of the pendulums can be expressed as

$$T_2 = \frac{1}{2} m (\dot{y} + r\dot{\theta} \sin \theta)^2 + \frac{1}{2} m (r\dot{\theta} \cos \theta)^2 \quad (2)$$

where m is the mass of the two pendulums, r is the radius of the pendulums.

With respect to the center of the ball considered to be the point of zero potential, the potential energy of the system is

$$V = -mgr \cos \theta \quad (3)$$

The Lagrange function can be express as

$$L = T_1 + T_2 - V \quad (4)$$

According to Lagrange equations

$$\frac{d}{dt} \left(\frac{\partial L}{\partial \dot{q}_j} \right) - \frac{\partial L}{\partial q_j} = Q_j \quad (5)$$

The dynamics of the linear motion can be written as

$$\begin{cases} (m + 2M)\ddot{y} + mr\ddot{\theta} \cos \theta - mr\dot{\theta}^2 \sin \theta = \frac{\tau}{R} \\ m\dot{y}r \cos \theta + mr^2\ddot{\theta} + mgr \sin \theta = \tau \end{cases} \quad (6)$$

This dynamic function is not integrable, but provides the basis for trajectory planning that can make the system controllable from an initial configuration to a desired configuration in practical application.

B. Smooth trajectory planning of linear motion

The smooth trajectory planning from an initial configuration to an expected final configuration is essential to the robot, which can enhance the performance of linear motion. The dynamic function given by (6) can be rearranged as

$$\begin{aligned} \ddot{y} &= f(\theta, \dot{\theta}, \ddot{\theta}) \\ &= \frac{mgr \sin \theta + mr \sin \theta R \dot{\theta}^2 + (mr^2 - mr \cos \theta R) \ddot{\theta}}{(m + 2M)R - mr \cos \theta} \end{aligned} \quad (7)$$

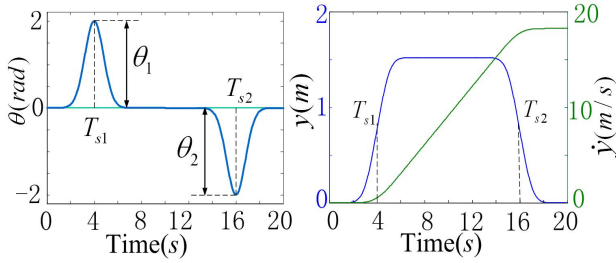
The coefficients of the terms related to θ in (7) are constant terms. This indicates that in linear motion, in order to keep a desired uniform speed ($\dot{y} = 0$) of the robot, the pendulums should be maintained on the vertical position ($\dot{\theta} = 0$, $\ddot{\theta} = 0$, $\sin \theta = 0$). The nonzero tilt angle of the pendulums may activate the robot to accelerate. It is also implied that the desired velocity of the robot in linear motion can be obtained by given the proper tilt angle, that is, the position of the robot is controllable.

The whole process of linear motion from initial static configuration to final static configuration is divided to three stages, which are starting stage, uniform motion stage and stopping stage. The corresponding curve of velocity \dot{y} should fit to the ladder diagram. From the starting stage to uniform motion stage, the velocity \dot{y} accelerates from zero to a desired uniform velocity \dot{y}_d , so the pendulums should be rotated to the desired angle θ_d first, then lean back to the vertical position (Fig. 4(a)). With the realization of these features of the system of linear motion, inspired by [11] and [12], a smooth trajectory for tilt angle of the pendulums based on normal distribution function is proposed by (8):

$$\theta(t) = \theta_1 e^{-\mu_1(t-t_{s1})^2} + \theta_2 e^{-\mu_2(t-t_{s2})^2} \quad (8)$$

where θ_1 and θ_2 are the amplitudes of the normal distribution function, t_{s1} and t_{s2} are the time the tilt angle reaches the peak, μ_1 and μ_2 are the constant scalars. The constant scalars μ_1 and μ_2 determine the width of the normal distribution function. Regulation of these parameters can change the state of the robot in linear motion.

Numerically solved by MATLAB, the curve of tilt angle of pendulums is shown in Fig. 4(a). The robot is controlled from the initial static configuration to the final static configuration through the smooth trajectory. Fig. 4(b) is the velocity and displacement of the sphere under the action of the pendulums. The accelerating state, uniform speed motion stage and decelerating stage are described clearly.



(a) Tilt angle of pendulums (b) Velocity and displacement of sphere
Fig. 4. Smooth trajectory planning for linear motion

C. Feedback controller for linear motion

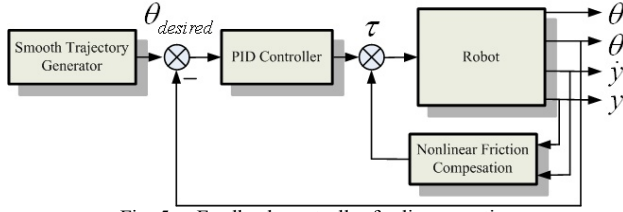


Fig. 5. Feedback controller for linear motion

The smooth trajectory planning method is theoretically proposed. Actually, the unexpected noise from floor condition, uncertain friction between sphere and floor and mechanical error may disturb the state of the robot. A feedback controller is designed to ensure the accurate trajectory planning for the system. The diagram of the controller is shown in Fig. 5. The desired tilt angle θ_d is regulated by function (8). The controller feeds back the practical tilt angle θ and outputs the torque τ of the motor shafts actuated on the pendulums. A nonlinear friction compensation model is added to adjust the torque. The friction model is composed of viscous damping friction term and impact force term which are related to the velocity of the sphere and displacement of the sphere respectively.

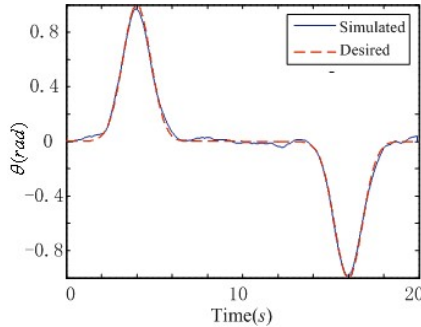
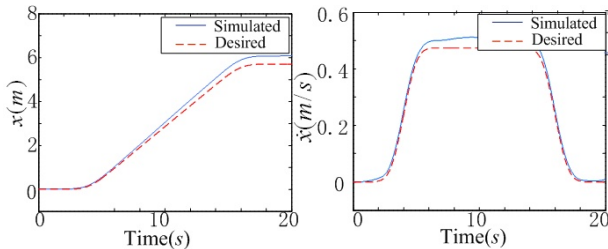


Fig. 6. Tilt angle



(a) Displacement of the sphere (b) Velocity of the sphere
Fig. 7. Angle of the sphere in simulation

The controller is verified by simulation. Given the value of the parameters, $\theta_1=1$, $\theta_2=-1$, $\mu_1=\mu_2=0.8$, $t_{s1}=4$, $t_{s2}=16$,

the simulation time is 20s, the planned tilt angle θ tracks the desired angle θ_d as shown in Fig. 6. The solid curve is the tilt angle in simulation and the dashed line is the desired angle.

The effect of the feedback controller can be found in Fig. 7. The displacement and velocity of the robot output from the controller in simulation are shown in Fig. 7(a) and Fig. 7(b) respectively. The feedback controller is capable to control the robot to move linearly in the expected motion under the disturbance from the floor.

D. Prototype experiment of linear motion



Fig. 8. Linear motion experiment

The linear motion experiment is done in the indoor environment in order to minimize the disturbance from the floor. The smooth trajectory planning was implemented on the prototype. The two pendulums are controlled to rotate synchronically to ensure the linear route. As shown in Fig. 8, the robot moves from the initial static configuration to the final static configuration by the tilt of the pendulums. The tilt angle of the pendulums is calculated by integrating the angular velocity of the sphere and data measured by encoders of the motors. The curve of tilt angle is plotted in Fig. 9. It can be concluded that the practical curve of tilt angle coincides with the smooth trajectory planning in theory.

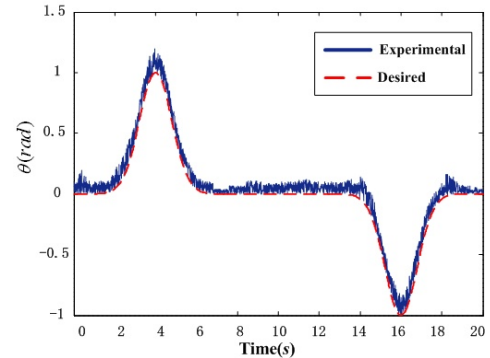
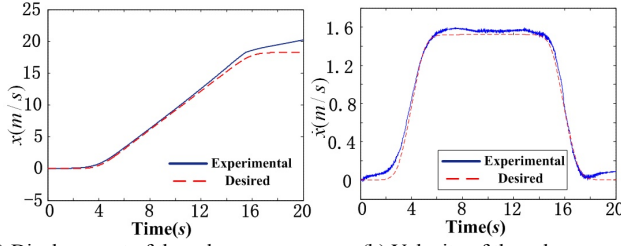


Fig. 9. Tilt angle in experiment

The displacement and velocity of the robot in experiment are shown in Fig. 10. The velocity of the sphere in Fig. 10(b) is measured by the angular rate sensor, and the data of displacement is obtained by integration of the data of velocity. The noise on the curves may come from the sensitivity of the angular rate sensor and the condition of the

floor. It can be concluded that the motion state of the sphere coincides with the smooth trajectory planning.



(a) Displacement of the sphere (b) Velocity of the sphere
Fig. 10. Angle of the sphere in experiment

IV. TURNING IN PLACE CONTROL

Some spherical robots have featured turning in place motion, which can enhance the mobility and tolerance of hostile environment. This motion exists in the spherical robots which belong to statically stable system, such as rotor type, car type and pendulum type. The turning in place motion has not been proposed separately as a definite motion in previous study, which should not be neglected as one of motion characteristics of spherical robots.

A. Dynamics of turning in place motion

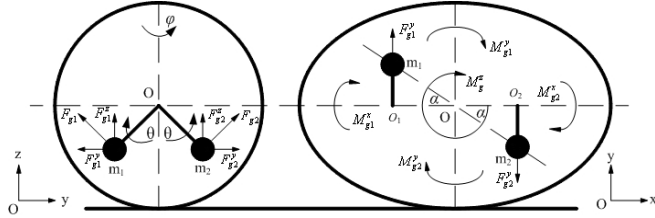


Fig. 11. Model of turning in place

The model of turning in place motion is shown in Fig. 11. The major axis is simplified as a rod fixed to the sphere. The two pendulums can only rotate about the x axis on the endpoints of the rod O_1 and O_2 . When the two pendulums rotate synchronously to opposite direction, the eccentric moment about the x and y axes and the inertia force along the z axis are in equilibrium. The force condition of turning in place motion is given by

$$\begin{aligned} \sum F_x &= 0 \\ \sum F_y &= F_{g1}^y - F_{g1}^y = 0 \\ \sum F_z &= F_{g1}^z + F_{g2}^z - G + N = 0 \\ \sum M_x &= M_{g1}^x - M_{g2}^x = 0 \\ \sum M_y &= M_{g1}^y - M_{g2}^y = 0 \\ \sum M_z &= M_g^z - M_f \end{aligned} \quad (9)$$

It can be concluded that the sphere is actuated only by the inertia moment about z axis generated by the inertia forces along y axis, so the sphere can only roll about z axis in theory, which is turning in place.

The motions of the sphere and two pendulums can not be projected to one plane, so the dynamics of turning in place motion is derived on the theorem of moment of momentum. The motion of one pendulum can be decomposed to one rotation about the rod in vertical plane $yozy$ and one rotation

about the z axis in horizontal plane xoy . So the velocity of one pendulum can be written as

$$\begin{cases} V_r = r\dot{\theta} \\ V_d = r'\dot{\varphi} \end{cases} \quad (10)$$

where V_r is the linear velocity of pendulum about x axis, V_d is the linear velocity about z axis, θ is the rotation angle of the pendulums about the rod, φ is the rotation angle of the robot about z axis, and $r' = \sqrt{d^2 + r^2 \sin^2 \theta}$ is the rotation radius about z axis.

The projection of the two velocities in (10) in the orthogonal plane can be expressed as

$$V_{\perp} = r\dot{\theta} \cos \theta \cos \alpha - r'\dot{\varphi} \quad (11)$$

where α is the acute angle between the rod and the line connecting the two canroids of the pendulums on top view.

The moment of momentum of the system is given by

$$L_z = 2mr'(r\dot{\theta} \cos \theta \cos \alpha - \frac{d}{\cos \alpha} \dot{\varphi}) - J\dot{\varphi} \quad (12)$$

According to the theorem of moment of momentum, the equivalent friction moment can be calculated by

$$M_f = \frac{d}{dt} \left(2mr'(r\dot{\theta} \cos \theta \cos \alpha - \frac{d}{\cos \alpha} \dot{\varphi}) - J\dot{\varphi} \right) \quad (13)$$

The dynamics of turning in place motion is given by

$$2m d r \dot{\theta} \cos \theta - 2m \frac{d^2}{\cos^2 \alpha} \dot{\varphi} - J \dot{\varphi} = \int_0^t M_f dt \quad (14)$$

where $\frac{d^2}{\cos^2 \alpha} = \frac{d^2}{\cos^2(\tan^{-1}(\frac{r \sin \theta}{d}))}$.

The coupling trigonometric item is simplified by

$$\cos^2 \left(\tan^{-1} \left(\frac{r \sin \theta}{d} \right) \right) \approx k \cos 2\theta + b \quad (15)$$

The fitting coefficient k and b are determined by the structure parameters r and d .

So the dynamic function can be simplified as

$$2m d r \dot{\theta} \cos \theta - \frac{2m d^2}{(k \cos 2\theta + b)} \dot{\varphi} - J \dot{\varphi} = \int_0^t M_f dt \quad (16)$$

The relationship between φ , θ and M_f is given by

$$\varphi = \frac{m d r}{\sqrt{P(P+Q)}} \text{Ln} \left| \frac{\sin \theta(t) + \sqrt{\frac{P+Q}{2Q}}}{\sin \theta(t) - \sqrt{\frac{P+Q}{2Q}}} \right| - \int_0^t \frac{M_f dt}{J + 2m d^2 (k \cos 2\theta + b)} \quad (17)$$

where P and Q are the constant terms once the k and b are determined, $P = J + 2b m d^2$, $Q = 2k m d^2$.

The dynamic equation (17) can not be solved by analytical method, but is essential for verifying the effectiveness of the stick-slip control method.

B. Stick-slip control of turning in place motion

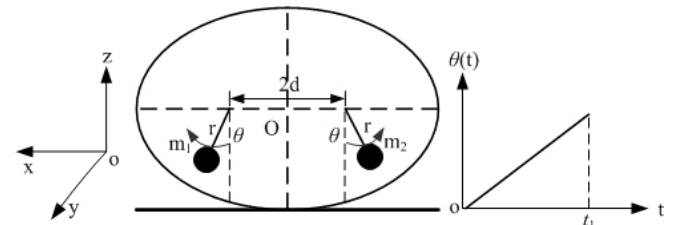


Fig. 12. Stick stage model

The stick-slip control method is proposed for turning in place motion, which can be divided into stick stage and slip stage. In initial state, the sphere is static, and the pendulums are in vertical position with no power supplement. Fig. 12 is the stick stage model of turning in place motion. The two pendulums are rotated in a same angular velocity but opposite direction. The inertia moment generated by inertial force of the acceleration of pendulums at the time t_{0+} is insufficient to activate the sphere, that is, the sphere is kept static by the static friction moment. The angle θ increases to a certain value slowly with time t until the time t_1 .

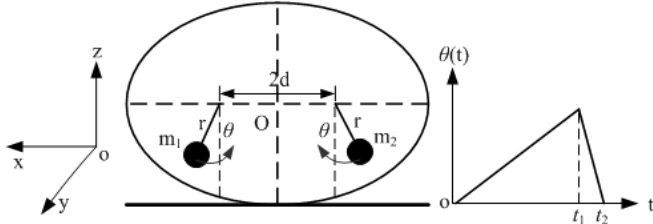


Fig. 13. Slip stage model

The slip stage is shown in Fig. 13. The pendulums are rotated to angle θ of opposite direction at the time t_1 . In slip stage, the pendulums are controlled back to the vertical position rapidly in a short interval. The sphere is actuated to turn in place by the inertia moment generated by inertia force of large acceleration of pendulums, that is, the friction moment is weak compared with inertia moment in slip stage. When the pendulums return back to vertical position at the time t_2 , the power supplement to motors is off. Then the sphere will stop when the kinetic energy is exhausted by the friction moment. The two stages constitute one step of the turning in place motion.

C. Simulation of stick-slip control

Considered the complexity of the dynamics of turning in place motion, relationship between the parameters is solved by simulation. The system parameters of robot in simulation given in TABLE I are experimentally determined.

TABLE I
PARAMETERS OF TURNING IN PLACE IN SIMULATION

| Symbol | Quantity | Value |
|--------|---------------------------------|-------------------------|
| M | mass of the sphere | 0.95 kg |
| m | mass of one pendulum | 0.35 kg |
| J | moment of inertia of the sphere | 0.0029 kgm ² |
| r | radius of pendulums | 0.038 m |
| d | half length of the rod | 0.045 m |
| k | fitting coefficient | -0.3082 |
| b | fitting coefficient | 1.3082 |

The friction model in simulation is given by

$$M_f = \begin{cases} D_v \dot{\varphi} \text{sign}(\dot{\varphi}), & \dot{\varphi} \neq 0 \\ M_{static}, & \dot{\varphi} = 0 \end{cases} \quad (18)$$

where M_{static} is the static friction moment, D_v is the viscous damping coefficient. The value is tested by experiment on flat indoor floor, $M_{static}=0.01424\text{Nm}$, $D_v=0.057\text{Nms/rad}$.

The tilt angle θ is controlled by

$$\theta(t) = \begin{cases} -\frac{\theta_m}{K_v} \cos(\omega t) + (1 - \frac{1}{K_v})\theta_m & \text{stick} \\ \frac{\theta_m}{K_v} \cos(K_f \omega t) + (1 - \frac{1}{K_v})\theta_m & \text{slip} \end{cases} \quad (19)$$

where θ_m is the maximum value of tilt angle, ω is the harmonic frequency, K_v is the angular velocity coefficient which dominates the angular velocity of pendulums, K_f is the frequency coefficient which can change the time proportion of slip stage in one step to regulate the value of inertial force. The value of parameters in (19) are given, $\theta_m = \pi/3$, $\omega = \pi/0.8$, $K_v=2$, $K_f=4$.

Fig. 14 is the results of the simulation. The solid line and dashed line are experimental results and desired values respectively. The time of one step of stick-slip process is 1s. In simulation, the noise from uncertain factors is added to the model. The equivalent friction moment is sufficient in simulation to keep the robot static in stick stage. The tilt angle displacement of one pendulum is shown in Fig. 14(a). The two pendulums are controlled to rotate periodically to an opposite direction. The slowly rising curve of tilt angle is the stick stage, the robot is static, and so the corresponding body turning angle is zero. The suddenly falling curve is the slip stage, the robot turns about the vertical axis to a certain angle by the inertia moment generated by the acceleration of the pendulums as shown in Fig. 14(b).

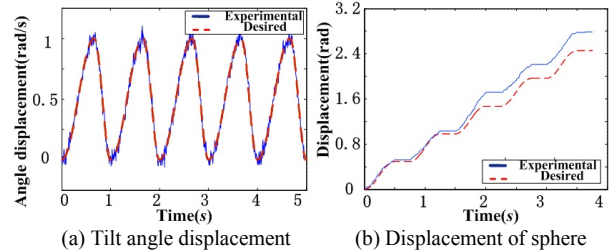


Fig. 14. Simulation of turning in place motion

D. Prototype experiment of turning in place motion



Fig. 15. Experiment of turning in place motion

The stick-slip principle is verified in experiment of turning in place motion. The two pendulums are controlled to the opposite direction. The robot can only rotate about vertical axis without rolling in theory, so the tilt angle is the angle the motor shafts rotate through. As shown in Fig. 15,

the robot can continuously turn in place by the repeated input of the two stages of stick-slip principle. The robot can orient to the desired direction through the regulation of the amplitude of the tilt angle of the two pendulums.

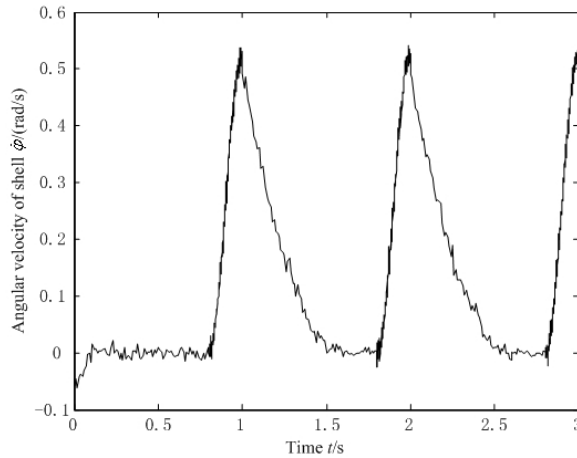


Fig. 16. Angular velocity of the robot

The angular velocity of the robot about vertical axis is shown in Fig. 16. The curve is like sawtooth wave. In the first stick stage, the angular velocity is negative because in initial stage, the instantaneous momentum conservation occurs between the sphere and the pendulums, the turning angle and the inertia moment of pendulums are to the opposite direction. It can be found that in experiment, the turning angle of the sphere is not zero in stick stage. The reason is that the friction moment is insufficient to stop the robot immediately.

V. CONCLUSION

A spherical robot of new drive mechanism is studied in this paper. The linear motion and turning in place motion control of a two pendulums driven spherical robot are studied in this paper. The emphasis of linear motion control is placed on the movement to a desired configuration. The relationship between dynamic parameters is found based on the dynamic equation. The smooth trajectory planning method for linear motion based on normal distribution function is proposed. A feedback controller is constructed for the accurate trajectory planning. The tilt angle and sphere displacement in simulation and experiment represent accordance with the expectation. The robot can be controlled to move from an initial static configuration to a final static configuration through the adjustment of parameter. To enhance the mobility of the robot, a stick-slip control method is proposed for turning in place motion. The dynamics deduced on the theory of moment of momentum provides the basis for validating the principle. The two stages of one step are interpreted in detail. The principle is verified by simulation. In prototype experiment, the robot can continuously turn in place to a desired angle.

REFERENCES

- [1] Y. S. Xu and S. K. Au, "Stabilization and path following of a single wheel robot," *IEEE trans. Mechatronics*, vol. 9, no.2, pp. 407–419, Jun. 2004.
- [2] A. Halme, T. Schonberg, Y. Wang, "Motion control of a spherical mobile robot," *IEEE International Workshop on Advanced Motion Control, AMC*, vol.1, pp.259–264, 1996.
- [3] R. H. Armour and J. F. V. Vincent, "Rolling in Nature and Robotics: A Review," *Journal of Bionic Engineering*, vol.3, no.4, pp.195–208, Dec. 2006
- [4] F. Michaud and S. Caron, "Roball, the rolling robot," *Autonomous Robots*, vol. 12, no. 2, pp. 211–222, Mar. 2002.
- [5] Q. Zhan, C. Jia, X. H. Ma and Y. T. Zhai, "Mechanism Design and Motion Analysis of A Spherical Mobile Robot," *Chinese Journal of Mechanical Engineering*, vol.18, no. 4, pp.542–545, Dec. 2005.
- [6] M. Seeman, M. Broxvall, A. Saffiotti and P. Wide, "An autonomous spherical robot for security tasks," *Proceedings of the 2006 IEEE Int. Conf. Computational Intelligence for Homeland Security and Personal Safety*, pp. 51–55, Oct. 2006.
- [7] S. Bhattacharya and S. K. Agrawal, "Spherical Rolling Robot: A Design and Motion Planning Studies," *IEEE trans. Robotics and Automation*, vol. 16, pp.835–839, 2000.
- [8] R. Mukherjee, M. A. Minor and J. T. Pukrushpan, "Motion Planning for a Spherical Mobile Robot: Revisiting the Classical Ball-Plate Problem," *Journal of Dynamic Systems, Measurement and Control, Transactions of the ASME*, vol. 124, pp. 502–511, Dec. 2002.
- [9] T. Das and R. Mukherjee, "Reconfiguration of a Rolling Sphere: A Problem in Evolute-Involute Geometry," *Journal of Applied Mechanics, Transactions ASME*, vol. 73, no. 4, pp. 590–597, Jul. 2006.
- [10] T. Otani, T. Urakubo, S. Maekawa and H. Tamaki, "Position and Attitude Control of a Spherical Rolling Robot Equipped with a Gyro," *IEEE International Workshop on Advanced Motion Control, AMC*, pp. 416–421, 2006.
- [11] U. Nagarajan, A. Mampetta, G. A. Kantor and R. L. Hollis, "State Transition, Balancing, Station Keeping, and Yaw Control for a Dynamically Stable Single Spherical Wheel Mobile Robot," *2009 IEEE Int. Conf. Robotics and Automation*, Kobe, May. 2009, pp. 998–2003.
- [12] U. Nagarajan, G. Kantor and R. L. Hollis, "Trajectory Planning and Control of an Underactuated Dynamically Stable Single Spherical Wheeled Mobile Robot," *2009 IEEE Int. Conf. Robotics and Automation*, Kobe, May. 2009, pp. 3743–3748.